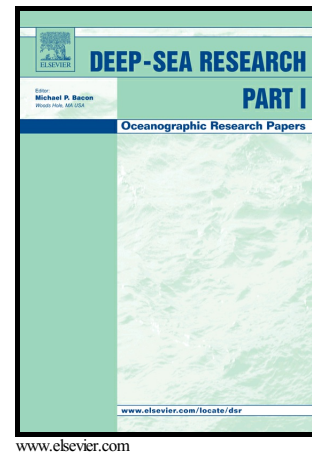


Author's Accepted Manuscript

Light comfort zones of mesopelagic acoustic scattering layers in two contrasting optical environments

Anders Røstad, Stein Kaartvedt, Dag L. Aksnes



PII: S0967-0637(15)30022-4
DOI: <http://dx.doi.org/10.1016/j.dsr.2016.02.020>
Reference: DSRI2611

To appear in: *Deep-Sea Research Part I*

Received date: 30 May 2015
Revised date: 8 February 2016
Accepted date: 9 February 2016

Cite this article as: Anders Røstad, Stein Kaartvedt and Dag L. Aksnes, Light comfort zones of mesopelagic acoustic scattering layers in two contrasting optical environments, *Deep-Sea Research Part I*, <http://dx.doi.org/10.1016/j.dsr.2016.02.020>

This is a PDF file of an unedited manuscript that has been accepted for publication. As a service to our customers we are providing this early version of the manuscript. The manuscript will undergo copyediting, typesetting, and review of the resulting galley proof before it is published in its final citable form. Please note that during the production process errors may be discovered which could affect the content, and all legal disclaimers that apply to the journal pertain.

1 Short Communication (Note)

2

3 Light comfort zones of mesopelagic acoustic scattering layers in two
4 contrasting optical environments

5

6 Anders Røstad¹, Stein Kaartvedt^{1,2}, Dag L. Aksnes^{3,*}

7

8 ¹Red Sea Research Center, King Abdullah University of Science and Technology, Thuwal
9 23955-6900, Saudi Arabia

10 ²Department of Biosciences, University of Oslo, PO Box 1066 Blindern, 0316 Oslo, Norway

11 ³Department of Biology, University of Bergen and Hjort Centre for Marine Ecosystem
12 Dynamics, Bergen N-5020, Norway

13 *Corresponding author: dag.aksnes@uib.no

14

15 Highlights

- 16 • Pronounced differences in the depth distributions of the acoustic scattering layers in the Red
17 Sea and Masfjorden can be accounted for by the difference in the water clarity.
- 18 • Light Comfort Zones (LCZ) and water clarity might be a predictor for changes in SL
19 distributions in space and time.
- 20 • Future studies of acoustic scattering layers should include accurate *in situ* light measurements
21 at mesopelagic depths.

22

23 ABSTRACT

24 We make a comparison of the mesopelagic sound scattering layers (SLs) in two contrasting
25 optical environments; the clear Red Sea and in murkier coastal waters of Norway (Masfjorden).
26 The depth distributions of the SL in Masfjorden are shallower and narrower than those of the Red
27 Sea. This difference in depth distribution is consistent with the hypothesis that the organisms of
28 the SL distribute according to similar light comfort zones (LCZ) in the two environments. Our
29 study suggest that surface and underwater light measurements ranging more than 10 orders of
30 magnitude is required to assess the controlling effects of light on SL structure and dynamics.

31

32 Keywords: Mesopelagic, Scattering layers, Vertical migration, Light

33

34 **1. Introduction**

35 Mesopelagic sound scattering layers (SLs), also called deep scattering layers, are ubiquitous
36 features of the oceans. SLs have received increased attention in recent years as they might
37 contain much higher biomass of mesopelagic fishes than previously assumed (Kartveit et al.,
38 2012; Irigoien et al., 2014). Since the first observations of SLs in the late 1940s (see references in
39 Fornshell and Tesei, 2013) it has been known that their characteristic diel vertical migrations
40 (DVM) are related to variations in the surface light. A common interpretation is that organisms
41 of the SL feed in the epipelagic at night and descend to mesopelagic depths to hide at daytime.
42 The daytime depth position, however, and consequently the vertical range of these migrations,
43 varies widely between locations. Bottom depth is one obvious constraint for the daytime depth
44 and its associated migration amplitude, but also hypoxia (Bianchi et al., 2013), temperature, and
45 density (Cade and Benoit-Bird, 2015) have been associated with SL distributions. Several

46 previous studies also suggest that the SL organisms might have preference for a range of light
47 intensities that typically span some orders of magnitude (Roe, 1983; Staby and Aksnes, 2011;
48 Prihartato et al., 2015). Here, we elaborate this idea and present the first evidence that this might
49 apply to the observed SLs in two very different optical environments

50

51 **2. Theory and expectations**

52 Organisms that have the ability to actively avoid too strong and too low light intensities can be
53 said to occupy a light comfort zone, LCZ (Dupont et al., 2009). This differs somewhat from the
54 isolume concept where organisms are assumed to be attracted by a specific light intensity (Cohen
55 and Forward, 2009). It might be speculated that the ultimate mechanism giving rise to a LCZ, e.g.
56 for mesopelagic fishes, represents the evolutionary solution to the trade-off conflict between
57 visual foraging opportunities and predation mortality (Clark and Levy, 1988; Rosland and Giske,
58 1994; Giske et al., 2013). Nevertheless and regardless of the ultimate cause, if SL organisms do
59 distribute according to a LCZ, two simple testable predictions emerge (Fig 1): A murky water
60 column (i.e. high light attenuation) is expected to have a shallower, and also narrower, SL depth
61 distribution than a clear water column. Here, we test these expectations by comparing the SLs
62 during a day in the clear Red Sea (clear water) with that of a murkier Norwegian coastal location,
63 Masfjorden.

64

65 **3. Methods**

66 *3.1. Study locations*

67 The DVM patterns of the organisms constituting the SLs of Masfjorden are dynamic and change
68 throughout the year in concordance with seasonal changes in light conditions and possibly the
69 distribution of prey (Staby et al., 2011; Dypvik et al., 2012a; Prihartato et al., 2015). Temperature

70 varies in upper waters, but is basically stable below 100 m (~7.5-8 C) throughout the year. High
71 latitudes are characterized by dusk summer nights with light intensities that can be higher than
72 the ambient day-time light of the SLs.

73 In contrast to Masfjorden, DVM patterns of the SLs in the Red Sea appear more or less
74 invariant throughout the year (cf. also Klevjer et al., 2012; Dypvik and Kaartvedt, 2013). This is
75 not surprising given the relatively small seasonal variations at this low latitude. Also, the Red Sea
76 is unique among the worlds' oceans in having very warm waters at depth (~21.5 °C all the way to
77 the bottom). Combined with presumably low prey concentrations, high metabolic rates related to
78 such warm waters appear to force the entire population of mesopelagic fish to make feeding
79 excursions to upper layers every night (Dypvik and Kaartvedt, 2013).

80 Here we present acoustic observations from the two locations at dates where light
81 measurements also were available; August 16, 2011 in Masfjorden (60°50'N 5°30'E) and
82 November 15, 2014 in the Red Sea (22°29'N, 39°02'E).

84 *3.2. Acoustic measurements*

85 In both locations, moorings with upward looking SIMRAD EK60 echosounders were deployed
86 on the bottom with the transceivers housed in pressure proof containers attached to a SIMRAD
87 38 kHz ES38DD transducer. Bottom depths at these locations were ~370 m in Masfjorden and
88 ~700 m in the Red Sea. In Masfjorden, the system was powered by cable to land, which also
89 transferred digitized data to a computer on shore. The cable was attached to a rope, which
90 secured retrieval of the rig at completion of the study (see Prihartato et al. 2015 for details)

91 The mooring deployed in the Red Sea was autonomous with a PC built into the same pressure
92 proof container as the acoustic transceiver and being powered by batteries in a separate pressure
93 proof container (system provided by METAS AS). The mooring was equipped with syntactic

94 foam for flotation and was deployed with a heavy concrete weight. The system was retrieved by
95 help of an acoustic release.

96 Echograms were visualized using Matlab. We made standard 24 h echograms as a function of
97 depth, but also as a function of the calculated ambient light (see 3.3). Acoustic values are given
98 as calibrated mean volume backscattering strength, S_v (dB re 1 m^{-1}).

99

100 *3.3. Light measurements*

101 At both locations measurements of underwater downwelling irradiance were obtained by a Trios
102 RAMSES ACC hyperspectral radiometer around mid-day down to depths of 275 m and 90 m for
103 the Red Sea and Masfjorden respectively. These measurements provided spectral resolution, with
104 3.3 nm bin size, of downwelling irradiance and were used to calculate ambient irradiance and to
105 estimate photon capture rate for a model organism at mid-day (see 3.4). At depths below the
106 deepest irradiance observation, we extrapolated by using attenuation coefficients (for each
107 wavelength bin) that were estimated from depths deeper than 100 and 50 m for the Red Sea and
108 for Masfjorden respectively.

109 In Masfjorden, measurements of total irradiance of the PAR band (400 -700 nm) just above
110 the surface were available from a LI-190 quantum sensor (at 15 minutes interval throughout day
111 and night. This sensor had sufficient sensitivity to measure night sky irradiance at this high
112 latitude in August and was, in combination with the estimated attenuation coefficient for PAR,
113 used to calculate underwater total irradiance through day and night in the 400-700 nm band, i.e.
114 without spectral resolution.

115 Similarly, for the Red Sea hourly integrated values of total broadband irradiance (W m^{-2}) were
116 available at a weather station located about 21 km from the location of acoustical registrations.
117 Comparison of this broadband registration with the simultaneous underwater measurement just

118 below the surface of the 400-700 nm band indicated a conversion factor of $1.16 \mu\text{mol quanta s}^{-1}$
119 W^{-1} , which was used to convert the total broadband irradiance measurements into total irradiance
120 in the 400-700 nm band. Unfortunately, the broadband sensor did not provide reliable
121 measurements of light intensity of the night sky.

122

123 *3.4. Calculation of total photon capture rate*

124 The brightness perceived by e.g. a fish can be approximated by total photon capture rates. We
125 calculated such rates for different depths at the two locations according to the procedure
126 described in Turner et al. (2009) for vision in lanternfish. This involved calculation of normalised
127 absorbance spectra (according to the 3.3 nm resolution of the hyperspectral radiometer used for
128 underwater light measurements) by the equations of Govardovskii et al. (2000, eq. 1-2). These
129 were converted into absolute spectral absorbance, by taking specific absorbance of rhodopsin
130 ($0.013 \mu\text{m}^{-1}$) and photoreceptor outer-segment ($50 \mu\text{m}$) into account (see Turner et al., 2009).
131 These data were then recalculated as spectral absorptance (eq. 6 in Turner et al., 2009), which
132 was multiplied by the estimated retinal irradiance (eq. 5 in Turner et al., 2009) to give an estimate
133 of the spectral photon capture rate at selected depths (see Table 1) at the two locations. Total
134 photon capture rate was obtained by summing over the entire spectrum. We assumed a peak
135 sensitivity of rod visual pigments of 487 nm which corresponds to an average of Myctophidae
136 listed in Douglas and Partridge (1997). This sensitivity was varied on the range 480 to 500 nm,
137 but provided relatively small changes (less than 10%) in calculated photon capture for all depths
138 at the two locations.

139

140 **4. Results**

141 *4.1. Light penetration*

142 The light penetration of the Red Sea and Masfjorden is illustrated in Fig. 2 for the 470 – 500 nm
143 band, which is relevant for deep see fish (Douglas et al., 1998). For the Red Sea the regression
144 estimates of $K_{470-500}$ were 0.0534 ± 0.0008 and $0.0366 \pm 0.0014 \text{ m}^{-1}$ shallower and deeper than
145 100 m respectively. For Masfjorden the estimates were 0.1920 ± 0.0057 , 0.0924 ± 0.0034 , and
146 $0.0596 \pm 0.0011 \text{ m}^{-1}$ for 0-25, 25-50, and below 50 m respectively (uncertainties are the estimated
147 95% c.i.). Thus, the light attenuation coefficients for the deepest layer were 61% higher in
148 Masfjorden than in the Red Sea. Extrapolation indicates that the light penetrations at the bottom
149 depths were similar, with a fraction of around 10^{-12} of the surface light, at the two locations.
150 Thus, despite a shallower bottom depth, the water column of Masfjorden appears to offer a
151 similar range of light intensities to the mesopelagic organisms as the Red Sea location.

152

153 *4.2. Acoustic registrations*

154 The upper 100 m of the Red Sea had relatively strong acoustic scatter in daytime as well as in
155 nighttime (Fig. 3A). Below this surface layer, we categorized the mesopelagic acoustic scatters
156 into three layers (Fig. 4A and Table 1). Layer 1 is located around 200 m depth at mid-day and
157 had a characteristic diel migration pattern (Fig. 3A). Below this layer there is a prominent
158 acoustic void that spans from 200 to about 320 m at mid-day. Layers 2 and 3 are distributed
159 between 320 – 480 m and 480 – 680 m depth respectively (Fig. 4A and Table 1). The depth
160 locations of the three layers change slightly throughout the day, becoming progressively deeper
161 until mid-day and shallower afterwards (Fig. 3A). In the afternoon the SL ascends rapidly into the
162 upper 100-200 m, remaining in upper waters throughout the night and descending rapidly next
163 morning. Only very few individual targets remained in the mesopelagic zone at night (layer 4 in
164 Fig. 3A).

165 In Masfjorden the shallowest layer 1 is seen around 80 – 120 m depth at mid-day (Fig 3A,
166 4B). The acoustic void extended from 120 to 170 m depth and layer 2 where located between 170
167 – 250 m. Nighttime depths were in the upper 25 m. A weaker layer 3, also migrating, occupied
168 the depth interval 250 – 380 m at mid-day, thereafter becoming progressively shallower until
169 ascending more rapidly to near-surface waters in the afternoon (Fig. 3B). Targets below 300 m
170 mostly remained at depth day and night (layer 4 in Fig. 3B).

171

172 *4.3. SL distribution in relation to variation in the surface light intensity*

173 In the lower panel of Fig. 3, we have replaced the depth axis with the total ambient irradiance as
174 calculated from the observed variations in surface PAR (see 3.3). While the SLs were more
175 shallowly distributed and more vertically compressed in Masfjorden, the ambient light of the SLs
176 and the acoustic void largely concurred (orders of magnitude) with that in the Red Sea (Table 1).
177 In association with the upward migration in the afternoon it appears as if ambient light of layer 2
178 and 3 increases two orders of magnitude in both locations (Fig. 3C and D). This might indicate
179 that the layers move upward faster than the reduction in incoming light. At dawn a similar,
180 although less pronounced, pattern is indicated. We note, however, that our calculations of
181 ambient irradiance are inaccurate, particularly during dusk and dawn. We assumed time-invariant
182 light attenuation and surface reflectance coefficients. In nature these coefficients are higher at
183 low sun angles and might therefore account for part of the increase in calculated ambient
184 irradiance during dusk and dawn. Finally, the organisms of the SLs might be sensitive for
185 variations in light at particular wavelengths that are not well reflected by variation in PAR.

186 At night time the combined layers 2 and 3 in Masfjorden occupied depths (upper 100 m, Fig.
187 3B) with ambient light similar to those observed at mid-day i.e. on the range $10^{-8} - 10^{-4}$ μmol

188 quanta $\text{m}^{-2} \text{s}^{-1}$ and with the strongest acoustic scatter (layer 2) on the range $10^{-5} - 10^{-4} \mu\text{mol}$
189 quanta $\text{m}^{-2} \text{s}^{-1}$ (Fig. 3D).

190 Measurements of night light were not available for the Red Sea (indicated with shaded area in
191 Fig. 3C). The calculated ambient night light of the mesopelagic SL was similar to the daytime
192 range when the surface irradiance was set constant at $10^{-4} \mu\text{mol quanta m}^{-2} \text{s}^{-1}$ (indicated with
193 shaded area in Fig. 3C). This value is about one order of magnitude lower than the light level of a
194 full moon (Jensen et al., 2001). At November 15 the moon was above the horizon after midnight
195 and was lit about 45%.

196

197 *4.4. Modelled photon capture rate*

198 The calculated photon capture rates reported in Table 1 indicate the brightness a lantern fish
199 (Myctophidae) perceive at mid-day. As shown by the ratio (last column of Table 1), the estimated
200 photon capture at the SL boundary depths are similar, i.e. within one order of magnitude, in the
201 Red Sea and Masfjorden. Although the wavelength composition was different at the two
202 locations (the Red Sea is "bluer", not shown), the percentage photons captured were similar with
203 ranges of 28 - 30% and 23 - 30% for different depths in the Red Sea and Masfjorden respectively.
204 Consequently, the variation in photon capture reflected largely the variation in the total ambient
205 irradiance as shown in Table 1 and Fig. 4C and D. A visual pigment sensitivity of 487 nm was
206 used for the values reported in Table 1. The exact value of this sensitivity, however, appears not
207 to be critical for the calculations. When this sensitivity was varied between 480 - 500 nm the
208 resulting photon captures varied less than 10% (not shown).

209

210 **5. Discussion**

211 The taxonomic compositions of the two systems have not been assessed for the days presented
212 here, and we briefly refer to knowledge from previous studies. In the most studied location,
213 Masfjorden, the lanternfish *Benthoosema glaciale* is the prevailing acoustic target in layer 3
214 (Kaartvedt et al., 2009, Dypvik et al., 2012b). The upper layers 1 and 2 are mainly composed of
215 juvenile and adult pearlside *Maruolicus muelleri* respectively (e.g. Giske et al., 1990; Staby et al.,
216 2011). Also in the Red Sea a lanternfish, *Benthoosema pterotum*, prevails at depth (layer 3)
217 (Klevjer et al., 2012; Dypvik and Kaartvedt, 2013). Catches in the Red Sea have been very scant;
218 likely due to avoidance (cf. Kaartvedt et al., 2012). Myctophids rapidly accumulate, however, in
219 the light beams of ROVs documenting their presence (Dypvik and Kaartvedt, 2013). Compared
220 to Masfjorden backscatter in the Red Sea is surprisingly strong, yet how this translates to
221 numerical abundance and biomass is unsettled as individual target strength (and the contribution
222 of possible resonance which may enhance the backscatter) remains to be established.

223

224 *5.1. Evidence of similar light comfort zones at the two locations*

225 Given the physical and biological differences between the two systems it is striking that the
226 calculated ambient irradiances of the acoustic layers, and also the estimated photon capture rates,
227 were not that different (Table 1). The two LCZ predictions (Fig. 1) are: The murkier Masfjorden
228 should have shallower, and also narrower, SL layers than the clear Red Sea. Quantitatively, this
229 prediction can be expressed $H \propto K^{-1}$ where H (m) is either the depth of the SL or the vertical
230 extension of the layer (Dupont and Aksnes, 2013). The reciprocal of the deepest $K_{470-500}$ (Fig. 2)
231 were 27.3 and 16.7 m for the Red Sea and Masfjorden respectively. This provides the LCZ
232 expectation that the SL of Masfjorden should be about 60% shallower, but also narrower, than the
233 SL of the Red Sea. The depth localization and thickness of the layers (Table 1) appear consistent
234 with this expectation. It is furthermore of interest that the thickness of the daytime “dead zone”

235 that was observed, i.e. the acoustic void between layer 1 and 2, is also shallower and narrower in
236 Masfjorden than in the Red Sea (Fig. 4 and Table 1).

237 The LCZ also implies that the daily SL variations within the two systems should disappear if
238 the sound scatters are plotted as a function of their ambient light instead of depth. During periods
239 around dusk and dawn, however, our results suggest that the ambient light of the organisms of the
240 SL increases markedly in both locations (Fig. 3C and D), which is not consistent with the LCZ
241 expectation. It has previously been speculated that such increased light exposure is governed by
242 higher predation risk taking by the SL organisms in order to increase own visual food intake in a
243 surface layer that is rich in prey organisms (e.g. Staby and Aksnes, 2011). As noted above,
244 however, the apparent increase in light exposure might, at least in part, be due to inaccurate
245 specification of underwater irradiance at low sun angles.

246 The results from Masfjorden indicate that the SL organisms expose themselves to similar light
247 intensities (Fig. 3D) day and night, i.e. the LCZ is the same. Whether this also applies for the Red
248 Sea and elsewhere needs to be addressed in future studies that measure spectral night light that
249 allows the assessment of photon capture rates.

250

251 *5.2. Recommendations for future studies*

252 The results reported here are based on a one day comparison. Future studies based on more
253 extensive data set, including seasonality as well as larger spatial coverage, are needed for a
254 general evaluation of LCZ behavior. Our study suggests that such studies require measurements
255 of irradiance levels that are much lower than commonly measured in biological oceanography.
256 Changes in irradiance at levels which are ten orders of magnitude lower than daylight, appear
257 significant to the organisms of the deepest SL. Night is often equated with dark in ecological
258 studies. As shown for Masfjorden, however, night light might provide the SL organisms with the

259 same ambient light they experience at daytime. Thus accurate characterization of variations in
260 night light, including spectral resolution enabling photon capture calculation, is needed to fully
261 characterize and understand the light governed behavior of mesopelagic organisms. Furthermore,
262 future studies should avoid the inaccuracies invoked in calculating underwater light from
263 measurements made in air, and rather strive to make continuous underwater measurements
264 ideally at the depths of the SL organisms. According to our results this requires sensors detecting
265 light intensities as low as 10^7 photons $m^{-2} s^{-1}$.

266

267 **Acknowledgements**

268 We would like to thank the Institute of Marine Research (IMR) for providing facilities for the
269 acoustic observations at Solheim in Masfjorden. Furthermore, we thank three anonymous
270 reviewers for valuable suggestions that improved our study. This study was funded by King
271 Abdullah University of Science and Technology, University of Oslo, and University of Bergen.

272

273 **References**

- 274 Bianchi D, Galbraith ED, Carozza DA, Mislán KAS, Stock CA (2013) Intensification of open-
275 ocean oxygen depletion by vertically migrating animals. *Nature Geosci* 6:545-548
- 276 Cade, D. E., and Benoit-Bird, K. J. 2015. Depths, migration rates and environmental associations
277 of acoustic scattering layers in the Gulf of California. *Deep Sea Research Part I:*
278 *Oceanographic Research Papers*, 102: 78-89.
- 279 Clark CW, Levy DA (1988) Diel Vertical Migrations by Juvenile Sockeye Salmon and the
280 Antipredation Window. *Am Nat* 131:271-290

- 281 Cohen JH, Forward RB, (2009) Zooplankton diel vertical migration – a review of proximate
282 control. In: Gibson RN, Atkinson RJA, Gordon JDM (eds) Oceanography and Marine
283 Biology: An Annual Review, Vol 47, p 77-109
- 284 Douglas RH, Partridge JC (1997) On the visual pigments of deep-sea fish. Journal of Fish
285 Biology 50: 68-85
- 286 Douglas RH, Partridge JC, Marshall NJ (1998) The eyes of deep-sea fish I: Lens pigmentation,
287 tapeta and visual pigments. Progress in Retinal and Eye Research 17:597-636
- 288 Dupont N, Aksnes DL (2013) Centennial changes in water clarity of the Baltic Sea and the North
289 Sea. Estuarine Coastal and Shelf Science 131:282-289
- 290 Dupont N, Klevjer TA, Kaartvedt S, Aksnes DL (2009) Diel vertical migration of the deep-water
291 jellyfish *Periphylla periphylla* simulated as individual responses to absolute light
292 intensity. Limnology and Oceanography 54:1765-1775
- 293 Dypvik E, Kaartvedt S (2013) Vertical migration and diel feeding periodicity of the skinnycheek
294 lanternfish (*Benthoosema pterotum*) in the Red Sea. Deep-Sea Research Part I-
295 Oceanographic Research Papers 72:9-16
- 296 Dypvik E, Klevjer TA, Kaartvedt S (2012a) Inverse vertical migration and feeding in glacier
297 lanternfish (*Benthoosema glaciale*). Marine Biology 159:443-453
- 298 Dypvik E, Rostad A, Kaartvedt S (2012b) Seasonal variations in vertical migration of glacier
299 lanternfish, *Benthoosema glaciale*. Marine Biology 159:1673-1683
- 300 Fornshell JA, Tesei A (2013) The Development of SONAR as a Tool in Marine Biological
301 Research in the Twentieth Century. International Journal of Oceanography 2013:9
- 302 Giske J, Aksnes DL, Balino BM, Kaartvedt S, Lie U, Nordeide JT, Salvanes AGV, Wakili SM,
303 Aadnesen A (1990) Vertical-Distribution and Trophic Interactions of Zooplankton and
304 Fish in Masfjorden, Norway. Sarsia 75:65-81

- 305 Giske J., Eliassen S, Fiksen O, Jakobsen,PJ, Aksnes DL, Jorgensen C, Mangel M (2013) Effects
306 of the Emotion System on Adaptive Behavior. *American Naturalist* 182: 689-703.
- 307 Govardovskii, VI, Fyhrquist N, Reuter T, Kuzmin DG, Donner K (2000) In search of the visual
308 pigment template. *Visual Neuroscience* 17: 509-528
- 309 Irigoien X, Klevjer TA, Røstad A, Martinez U, Boyra G, Acuña JL, Bode A, Echevarria F,
310 Gonzalez-Gordillo JI, Hernandez-Leon S, Agusti S, Aksnes DL, Duarte CM, Kaartvedt S
311 (2014) Large mesopelagic fishes biomass and trophic efficiency in the open ocean. *Nat*
312 *Communication* 5:3271, DOI: 10.1038/ncomms4271
- 313 Jensen HW, Durand F, Dorsey J, Stark MM, Shirley P, Premoze S (2001) A physically-based
314 night sky model. *Proceedings of the 28th annual conference on Computer graphics and*
315 *interactive techniques*. ACM, p 399-408
- 316 Kaartvedt S, Rostad A, Klevjer TA, Staby A (2009) Use of bottom-mounted echo sounders in
317 exploring behavior of mesopelagic fishes. *Mar Ecol Prog Ser* 395:109-118
- 318 Kaartvedt S, Staby A, Aksnes DL (2012) Efficient trawl avoidance by mesopelagic fishes causes
319 large underestimation of their biomass. *Mar Ecol Prog Ser* 456:1-6
- 320 Klevjer TA, Torres DJ, Kaartvedt S (2012) Distribution and diel vertical movements of
321 mesopelagic scattering layers in the Red Sea. *Marine Biology* 159:1833-1841
- 322 Prihartato PK, Aksnes DL, Kaartvedt S (2015) Seasonal patterns in the nocturnal distribution and
323 behavior of the mesopelagic fish *Maurolicus muelleri* at high latitudes. *Mar Ecol Prog Ser*
324 521:189-200
- 325 Roe HSJ (1983) Vertical distributions of euphausiids and fish in relation to light-intensity in the
326 Northeastern Atlantic. *Marine Biology* 77:287-298
- 327 Rosland, R., and Giske, J. 1994. A Dynamic Optimization Model of the Diel Vertical-
328 Distribution of a Pelagic Planktivorous Fish. *Progress in Oceanography*, 34: 1-43.

- 329 Staby A, Aksnes DL (2011) Follow the light—diurnal and seasonal variations in vertical
330 distribution of the mesopelagic fish *Maurolicus muelleri*. Mar Ecol Prog Ser 422:265-273
- 331 Staby A, Rostad A, Kaartvedt S (2011) Long-term acoustical observations of the mesopelagic
332 fish *Maurolicus muelleri* reveal novel and varied vertical migration patterns. Mar Ecol
333 Prog Ser 441:241-255
- 334 Turner JR, White EM, Collins MA, Partridge JC, Douglas RH (2009) Vision in lanternfish
335 (Myctophidae): Adaptations for viewing bioluminescence in the deep-sea. Deep-Sea
336 Research I 56: 1003-1017

337 Table 1. Approximate daytime SL thickness and depth boundaries. Layer refers to the numbers
 338 defined in Fig. 3 and 4. Void refers to the depth span between layer 1 and 2 characterized by low
 339 acoustic backscatter. The ambient irradiance (total number of photons summed over the
 340 spectrum) is given for the depths that correspond to the indicated layer boundaries. Total photon
 341 capture is modelled (see 3.4) from the ambient irradiance and vision related parameters set
 342 according to a myctophid (Turner et al. 2009). Ratio is the value obtained for the Red Sea divided
 343 by that for Masfjorden.

344

Layer	Layer thickness (m)		Layer boundary (m)		Ambient irradiance (photons m ⁻² s ⁻¹)			Total photon capture rate (photons m ⁻² s ⁻¹)		
	Red Sea	Mas-fjorden	Red Sea	Mas-fjorden	Red Sea	Mas-fjorden	Ratio	Red Sea	Mas-fjorden	Ratio
			140	80	8.7×10^{16}	1.5×10^{16}	6	2.4×10^{16}	3.4×10^{15}	7
1	60	40								
			200	120	6.3×10^{15}	9.2×10^{14}	7	1.8×10^{15}	2.4×10^{14}	8
Void	120	50								
			320	170	4.5×10^{13}	3.6×10^{13}	1	1.3×10^{13}	1.0×10^{13}	1
2	160	80								
			480	250	6.7×10^{10}	2.6×10^{11}	0.3	2.0×10^{10}	7.5×10^{10}	0.3
3	200	130								
			680	380	2.1×10^7	1.0×10^8	0.2	6.2×10^6	3.0×10^7	0.2

345

346

347

348 **Figures**

349 Fig. 1. Predictions from the LCZ hypothesis. If mesopelagic organisms distribute according to a
350 light comfort zone (LCZ), the depth distribution of the organisms in a murky water column will
351 be shallower and also narrower (H_2) than that of a clear water column (H_1). Both the depth
352 location and the extension of the vertical distribution are proportional to the reciprocal light
353 attenuation coefficient for downwelling irradiance which is given by the slope of the irradiance
354 curve (log-scale). Modified from Dupont and Aksnes (2013).

355
356 Fig. 2. Light penetration (given as the fraction of the irradiance just below surface) for the
357 wavelength band 470 – 500 nm in the clear Red Sea compared with that of the murkier
358 Masfjorden at the days of acoustic registrations; the Red Sea 15 November 2014 and Masfjorden
359 16 August 2011.

360
361 Fig. 3. Depth distribution of the acoustic scattering layers in the Red Sea on 15 November 2014
362 (A) and in Masfjorden on 16 August 2011 (B). The lower panels are based on the same
363 observations, but instead of depth show the calculated ambient irradiance (\log_{10}) of the acoustic
364 scatters for the Red Sea (C) and Masfjorden (D). The ambient irradiance ($\mu\text{mol quanta m}^{-2} \text{s}^{-1}$)
365 was calculated from the surface broadband (Red Sea) and PAR (Masfjorden) and the
366 corresponding K_{PAR} that were estimated from the underwater measurements at mid-day. We did
367 not have observations of surface irradiance at night for the Red Sea and this period is indicated by
368 grey shading in C.

369
370 Fig. 4. Mid-day depth distribution of acoustic scatter in the Red Sea (A, 15 November 2014) and
371 in Masfjorden (B, 16 August 2011). The lower panels are based on the same observations, but

372 instead of depth show the total ambient irradiance (photons $\text{m}^{-2} \text{s}^{-1}$), i.e. obtained by summin over
373 the measured spectrum, of the acoustic scatters of the Red Sea (C) and Masfjorden (D). Broken
374 lines indicate location of bottom. The numbers correspond to the layers that are also indicated in
375 Fig. 3 and Table 1.

376

377

Accepted manuscript

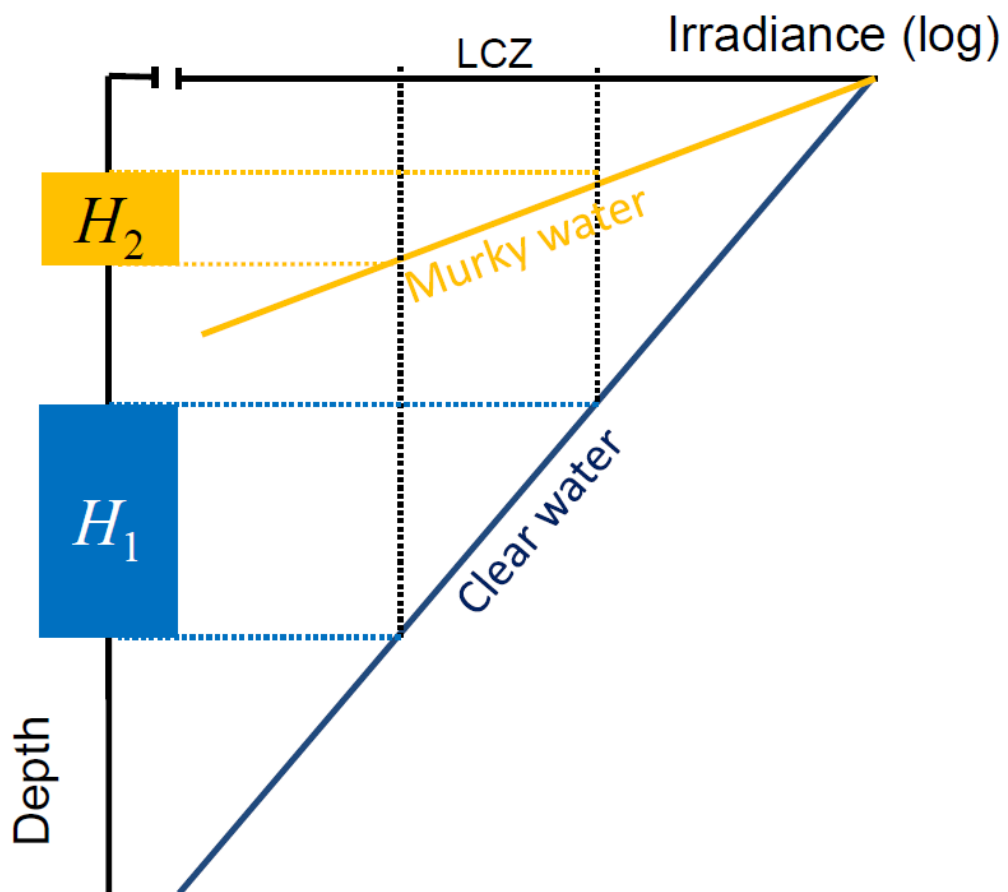


Fig. 1

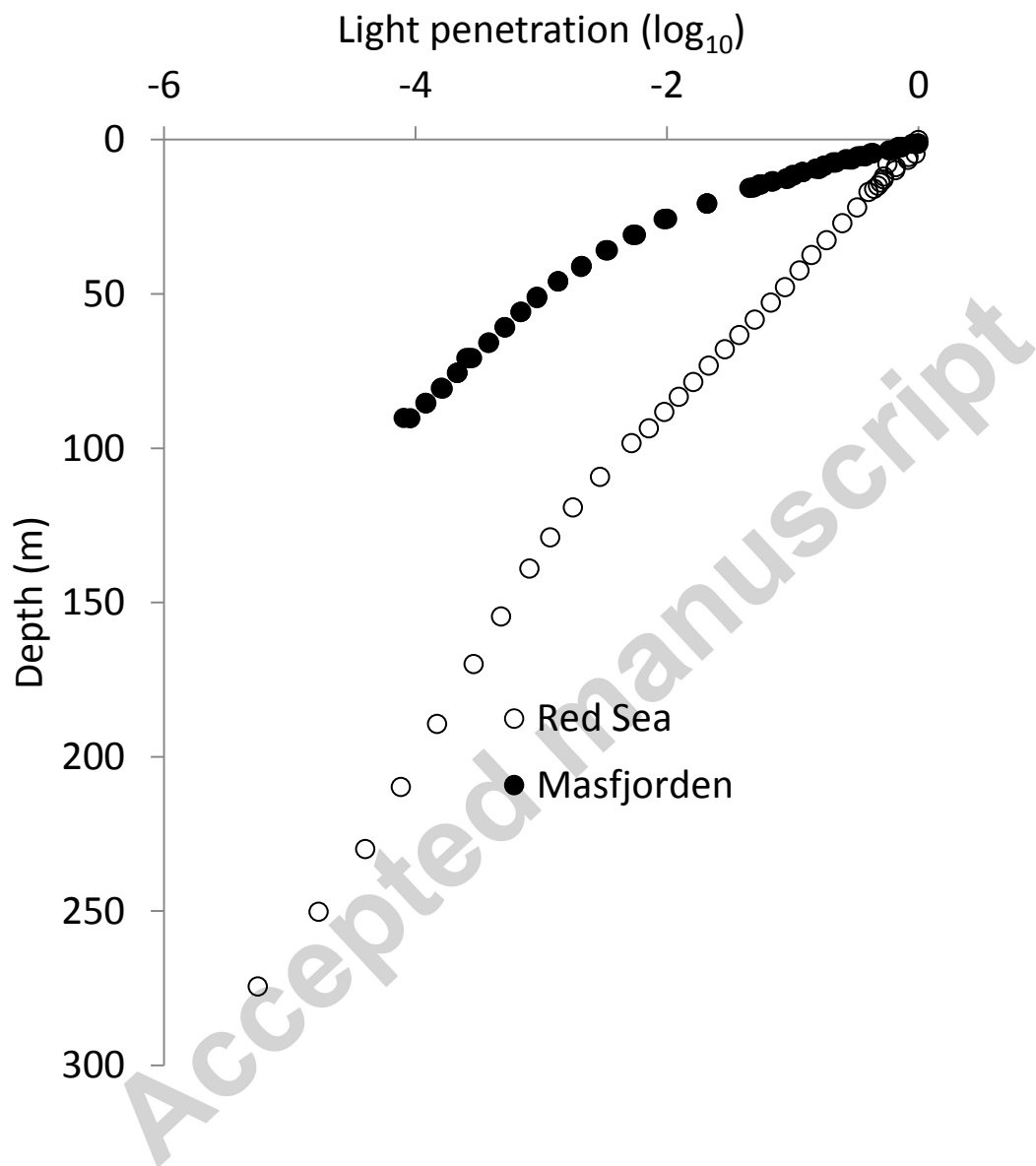


Fig. 2

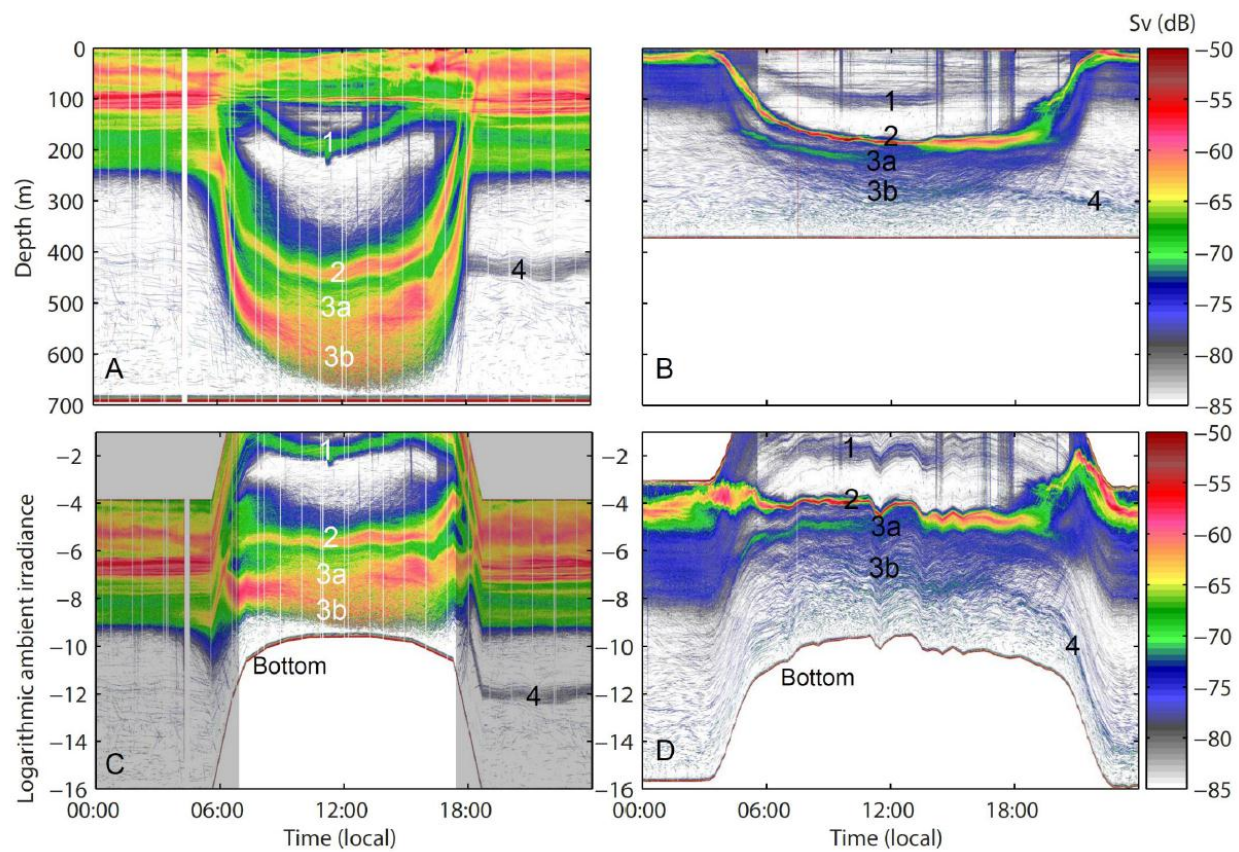


Fig. 3

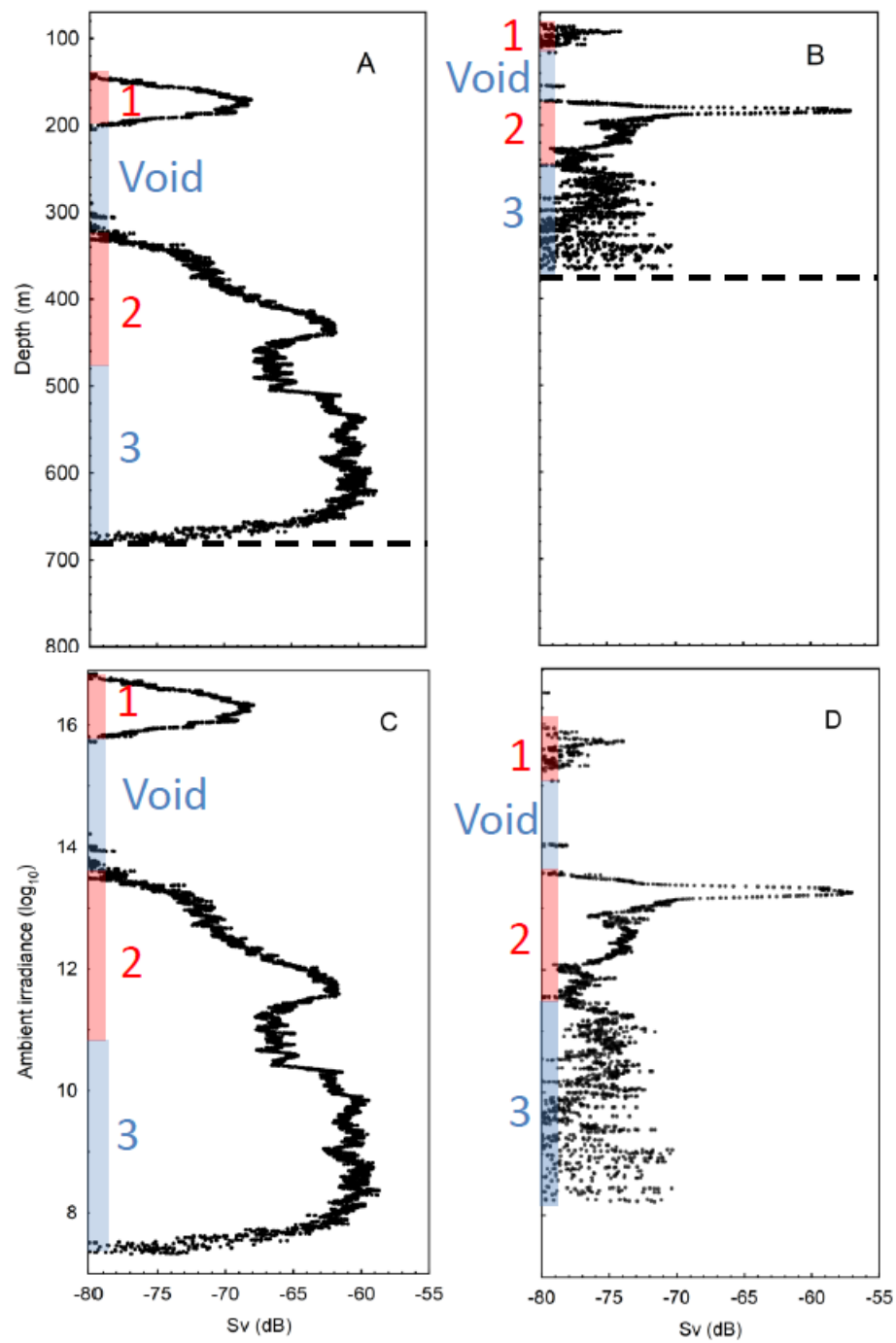


Fig. 4